

# Transparent cubic-ZrO<sub>2</sub> ceramics for application as optical lenses

Ulrich Peuchert<sup>a</sup>, Yoshio Okano<sup>a</sup>, Yvonne Menke<sup>a,\*</sup>, Steffen Reichel<sup>a</sup>, Akio Ikesue<sup>a,b</sup>

<sup>a</sup> SCHOTT AG, Hattenbergstrasse 10, D-55120 Mainz, Germany

<sup>b</sup> World Labo Co. Ltd., CSJ308, 1-2-19 Mutsuno, Atsuta-ku, Nagoya 456-0023, Japan

Available online 15 May 2008

## Abstract

Optical transparent polycrystalline ZrO<sub>2</sub> ceramics were fabricated by solid-state sintering process using first vacuum sintering followed by hot isostatic pressing. In the visible wavelength range (400–800 nm), the in-line transmittance of 5.6-mm thick samples reaches 68% at exemplary wavelength 600 nm (corresponding to an in-line absorbance based on 10 of  $A_{10} = 0.08 \text{ cm}^{-1}$ ), which is approximately 90% of theoretical limit. The refractive indices of the ZrO<sub>2</sub> optoceramics at 630 nm ( $n_d$ ) are varying between 2.10 and 2.20, depending on TiO<sub>2</sub> contents, the latter being used as sintering aid. The appearance of birefringence is strongly correlated to the addition of TiO<sub>2</sub> as sintering additive in the ceramic samples, whereas addition of TiO<sub>2</sub> and simultaneous increase in Y<sub>2</sub>O<sub>3</sub> content resulted in a decrease of birefringence.

© 2008 Elsevier Ltd. All rights reserved.

**Keywords:** ZrO<sub>2</sub>; Transparent; Optoceramics; Optical properties; Optical applications

## 1. Introduction

One of the main application fields of specialty glasses are lenses for objectives used in consumer, industrial as well as military optical systems. Due to the high compositional flexibility of the material glass a huge variety of lens materials can be realized at low costs in huge sizes tailored individually to a specific optical design. SCHOTT glass fulfils the optical design need in a variety of refractive indices, Abbe numbers, and partial dispersions as well as in high transmission.

However, increasing requirements from both sophisticated industrial as well as consumer mass markets have asked for optical transparent materials with extraordinary property combinations. For example the continuous trend to miniaturization of digital photographic devices like digital still cameras require optical materials with very high refractive indices up to 2.0 or higher whereas industrial devices like optical microscopes require materials with special dispersion characteristics. Here glass tends to its limits due to the fact, that compositions are needed that are prone to uncontrolled crystallization during cooling of the glass melt.

In contrast, transparent polycrystalline ceramics can address extraordinary property areas that glass cannot reach reliably.<sup>1,2</sup> By controlled sintering of suitable powders optoceramics of

high transmittance and high property homogeneity can be manufactured.<sup>3–5</sup> This has been first demonstrated in the field of active YAG-based ceramic laser materials.<sup>6</sup> Furthermore, Japanese companies have developed high refracting transparent ceramics made from cubic perovskite in qualities principally enabling the assembly as lenses into digital photographic devices.<sup>7</sup>

To our best knowledge, the first relevant reports concerning transparent c-ZrO<sub>2</sub> were published by Tsukuma (TOSOH CORP.), who studied the potential to make yttria-stabilized zirconia doped with TiO<sub>2</sub>.<sup>8,9</sup> TiO<sub>2</sub> is a standard agent for making non-transparent ceramics enabling very dense sintered bodies.<sup>10</sup> Transparent samples were demonstrated showing transmittance up to approximately 65% measured on a sample of only 0.76 mm thickness. There is no information available on the measurement technique used (in-line, integral, real in-line). More recent papers from TOSOH CORP. stresses effect of sintering temperature on the transparency of samples made from tetragonal stabilized zirconia (t-ZrO<sub>2</sub>).<sup>11</sup> In addition hypotheses for unusual optical properties that these samples exhibit are given based on phase transformation of t-ZrO<sub>2</sub> to c-ZrO<sub>2</sub>.

Clasen produced a c-ZrO<sub>2</sub> optoceramic via electrophoretic deposition with an in-line transmittance (including reflection losses) of 53% at 600 nm at a sample thickness of around 1 mm.<sup>12–14</sup>

According to Klimke and Krell<sup>14</sup> zirconia samples sized in the order of 30 mm × 50 mm have been manufactured via pressing, but also gel-casting has been tested. The samples were

\* Corresponding author.

E-mail address: [yvonne.menke@schott.com](mailto:yvonne.menke@schott.com) (Y. Menke).

manufactured in thicknesses between 2 and 6 mm, real-in-line-transmission (detection of transmitted light within  $0.5^\circ$  aperture angle; see Ref. [15]) values of a 4-mm thick sample are reported to be 75% of theoretical value (means approximately 57% or  $A_{10} = 0.32 \text{ cm}^{-1}$ ; data at 640 nm).

In the present paper both benefits and drawbacks of using transparent ceramics in optical lens systems are summarized. On the example of cubic stabilized zirconia, an alternative high refracting material system beside perovskites SCHOTT has been working on, the technological challenge to reach suitable qualities with increased thickness ready for bulk measurement of refractive index dispersion will be discussed.

## 2. Experimental

High purity cubic stabilized  $\text{ZrO}_2$  powder (TZ-10YS, TOSOH CORP., Japan) was used as starting material. The powder was mixed with specially prepared sintering aids containing  $\text{TiO}_2$  and binders and ball milled for 12 h in ethanol. Then, the alcohol solvent was removed by drying the milled slurry on a hot plate. The so-obtained powder was pressed with low pressure into required shapes in a metal mould and then cold isostatically pressed at 98 MPa.

Transparent ceramics made from cubic stabilized  $\text{ZrO}_2$  (c- $\text{ZrO}_2$ ) were obtained after sintering under vacuum ( $1 \times 10^{-3} \text{ Pa}$ ) at  $1650^\circ\text{C}$  for 3 h followed by hot isostatic pressing at  $1750^\circ\text{C}$  for 1 h at a pressure of 196 MPa. Because as-sintered samples were discolored into black due to the sintering in the reductive atmosphere, all the sample were heat-treated for oxidation in air at a temperature of around  $1000^\circ\text{C}$ . The preparation procedure of  $\text{ZrO}_2$  ceramic in this system is summarized in Fig. 1. The obtained optoceramic sample dimensions were 20 mm in diameter and 5–10 mm in thickness.

The refractive index  $n(\lambda)$  was measured by the prism coupling method<sup>16</sup> and V-Block measurement.<sup>17</sup>

The absorption spectra were measured in the wavelength range from 250 to 850 nm by means of a UV-vis-IR spectrophotometer using optically polished samples. The interaction of light with an optically transparent material is given by the addition of reflection, absorption, scattering and specular transmission (or in-line transmission after taking scattering into account).<sup>18</sup> The reflection losses are inherent to the material due to Snells law. An optimization of transmission is therefore only possible on scattering and absorption.

The total amount of light emerging from a material is termed as “total transmittance”, while it’s specularly transmitted portion is termed as in-line transmittance, after taking into account scattering as possible loss mechanism. Because inherent optical properties  $k$  are additive, and assuming that (1) small scattering and absorption  $(k_{\text{abs}} + k_{\text{scat}})d \ll 1$ , i.e. there is no diffusive light transport and (2) that light scattered once is not seen by the detector anymore, the absorption coefficient due to scatter can be calculated according to the following equation:

$$k_{\text{scatter}} = \frac{-\log(T_{\text{in-line}}/T_{\text{total}})}{d} = k_{\text{in-line}} - k_{\text{total}} \quad (1)$$

At the band edge this analysis cannot be made anymore, as assumption (1) is not valid anymore.

The birefringence of the optoceramics can be seen by using crossed nichols in a polarizing reflected light optical microscope.

Other properties of the material were evaluated by XRD, TEM/EDX and Raman scattering.

## 3. Results and discussion

In order to measure refractive indices and dispersion data with high accuracy, samples are needed that have sufficient quality and size. To reach the quality a suitable sinter additive is necessary. Besides  $\text{TiO}_2$ , which is a well-known sinter aid for high performance technical c- $\text{ZrO}_2$  ceramics,<sup>8,10</sup> additional chemical species have been added and resulted in low pore contents in the final ceramic.

In Fig. 2 the in-line transmission of  $\text{ZrO}_2$  optoceramics stabilized with 10 mol%  $\text{Y}_2\text{O}_3$  (Z10Y) containing different amounts of  $\text{TiO}_2$  (Z10Y–2 wt%  $\text{TiO}_2$  and Z10Y–5 wt%  $\text{TiO}_2$ ) is shown. Accordingly, the in-line transmission increased with increasing  $\text{TiO}_2$  content, up to 5 wt%  $\text{TiO}_2$  and reached a value of 51.6% at a wavelength of 600 nm for an 8.7-mm thick sample. It is obvious that the in-line transmission of the best sample of this study was drastically improved in comparison to those of the previously studies,<sup>8,9,12–14</sup> in which the in-line transmissions ranged from 1.2 to 40.3% after normalizing for the sample thickness of 8.7 mm. Nevertheless, in-line transmission of the 5 wt%  $\text{TiO}_2$  sample at 600 nm was still not sufficient for optical applications.

Another issue is homogeneity of optical properties. In a cubic transparent ceramic, the optical properties should be isotropic in all directions. Nevertheless, sinter additives and/or phase stabilizers may segregate at grain boundaries and cause fluctuations in optical properties. In Fig. 3 the birefringence observations of

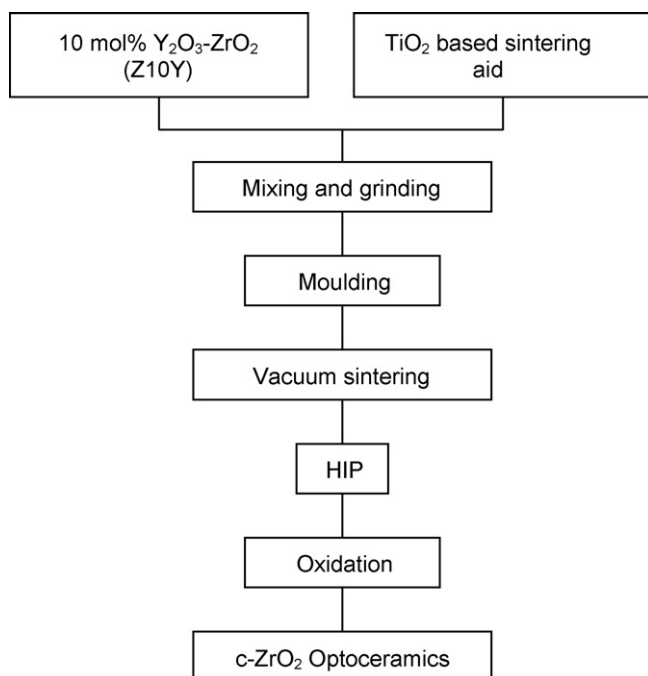


Fig. 1. Flow chart for preparation of c- $\text{ZrO}_2$  ceramics.

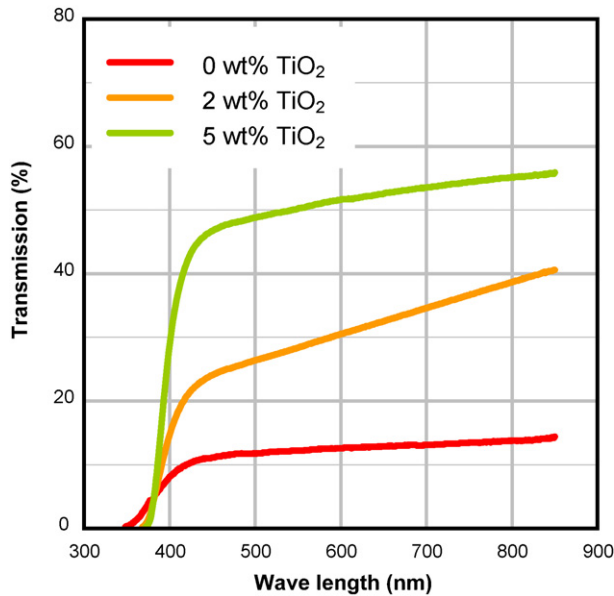


Fig. 2. In-line transmission of the samples of Z10Y–TiO<sub>2</sub> ceramics with different TiO<sub>2</sub> content. Transmission was measured on 6–9-mm thick specimen and normalized for the thickness of 8.3 mm.

the ceramic samples in the ZrO<sub>2</sub>–Y<sub>2</sub>O<sub>3</sub>–TiO<sub>2</sub> system are presented. It can be observed that the appearance of birefringence is significantly correlated to the TiO<sub>2</sub> content in the ceramic samples. With lower TiO<sub>2</sub> birefringence decreases, however on cost on transmission. There is thus a competition of transmission versus homogeneity. This competition can be due to structural features and/or can be process related.

### 3.1. Structural features influencing transmission and homogeneity

In order to understand the structural origin of the birefringence of the TiO<sub>2</sub>-containing c-ZrO<sub>2</sub>, micro-Raman scattering of the ZrO<sub>2</sub> ceramics has been carried out at several spots in the ceramic body. In Fig. 4 one exemplary spectrum out of 20 spectra carried out on different grains is shown and it is observed that the Raman spectra of the Z10Y–5 wt% TiO<sub>2</sub> ceramic is similar to the typical profile of TiO<sub>2</sub> free c-ZrO<sub>2</sub> (Z10Y–0 wt% TiO<sub>2</sub>). Besides the Raman bands observed in Z10Y–0 wt% TiO<sub>2</sub>, two supplementary bands are observed in Z10Y–5 wt% TiO<sub>2</sub>. One appears at 700 cm<sup>−1</sup> which can be assigned to a Ti–O bond. Another relatively small band appears at 470 cm<sup>−1</sup>.

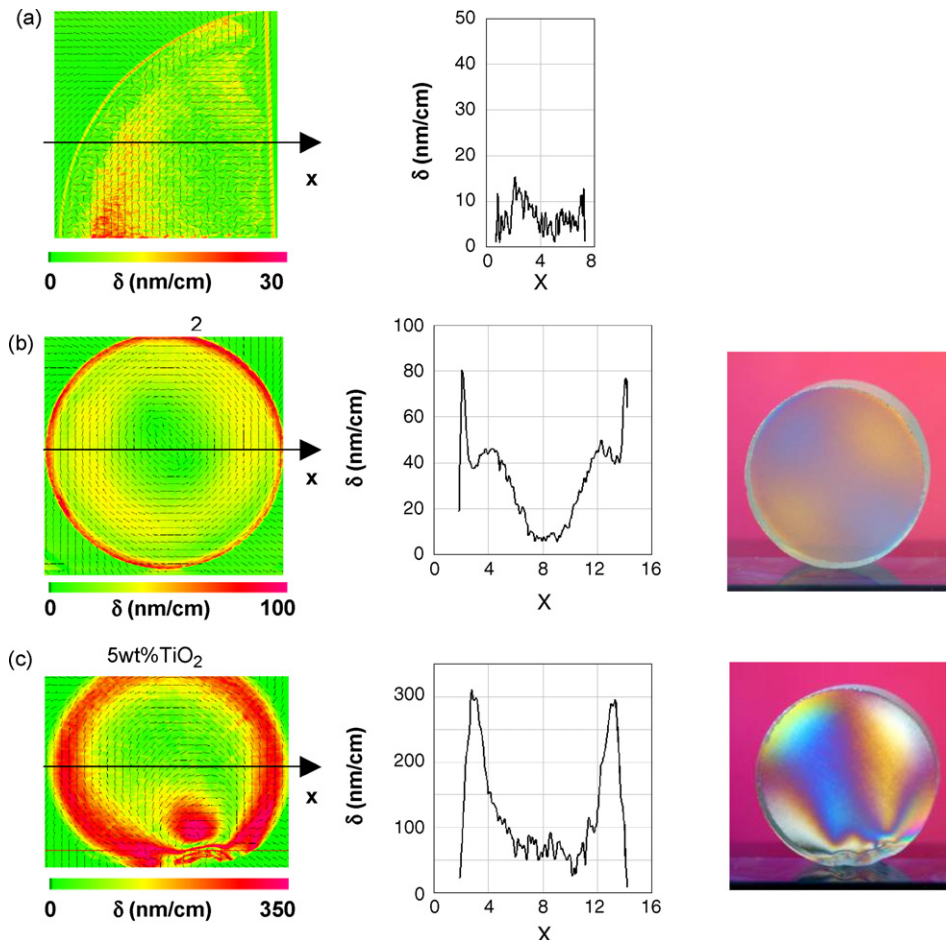
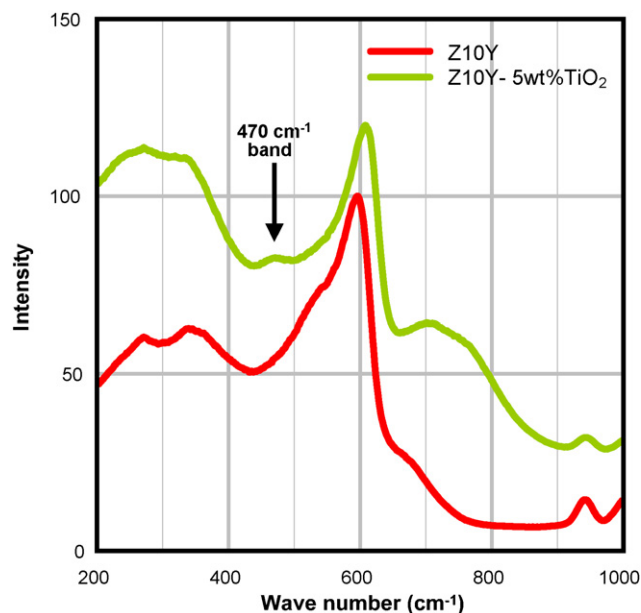
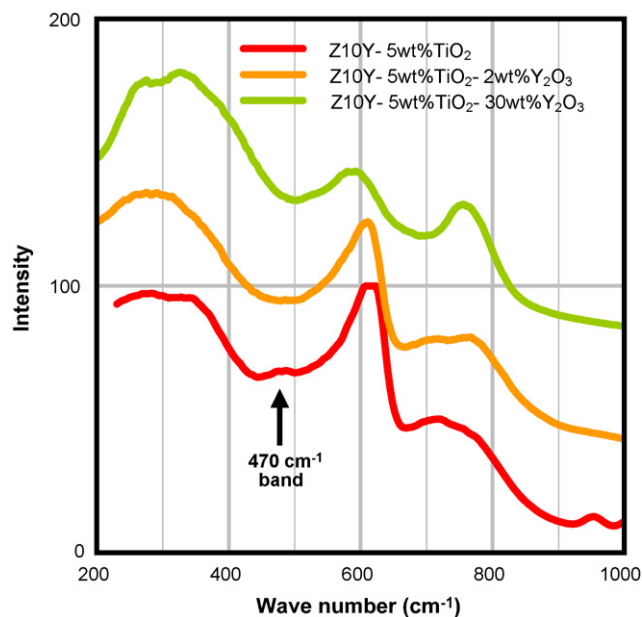


Fig. 3. Birefringence of the Z10Y–TiO<sub>2</sub> Ceramics. (a) Z10Y–0 wt% TiO<sub>2</sub>, (b) Z10Y–2 wt% TiO<sub>2</sub> and (c) Z10Y–5 wt% TiO<sub>2</sub>.

Fig. 4. Raman spectra of Z10Y ceramics and Z10Y–5 wt% TiO<sub>2</sub> ceramics.Fig. 6. Raman spectra of Z10Y–TiO<sub>2</sub> ceramics with increased Y<sub>2</sub>O<sub>3</sub> content.

This observed band at  $470\text{ cm}^{-1}$  in Z10Y–5 wt% TiO<sub>2</sub> is considered to be associated with oxygen displacement in the fluorite-type related structure. Oxygen displacement is a characteristic feature observed in t'-ZrO<sub>2</sub> ceramics, but it is well known that the t''-ZrO<sub>2</sub> phase which appears as metastable phase in the ZrO<sub>2</sub>–Y<sub>2</sub>O<sub>3</sub>-system by rapid quenching from melt and following annealing, shows this  $470\text{ cm}^{-1}$  band, i.e. characteristic band for oxygen displacement.<sup>19,20</sup> The unit cell of t''-ZrO<sub>2</sub> is cubic unlike for t-ZrO<sub>2</sub>, however oxygen ions displace as well as oxygen ions of t-ZrO<sub>2</sub> displace along *c*-axis (Fig. 5).

As the t''-ZrO<sub>2</sub> phase appeared via conventional solid-state reaction in the TiO<sub>2</sub>-containing system, it may be relatively stable. This is in contrast to the t'-ZrO<sub>2</sub> phase in the ZrO<sub>2</sub>–Y<sub>2</sub>O<sub>3</sub>-system without TiO<sub>2</sub>. Thus, TiO<sub>2</sub> might act as tetragonal phase, i.e. stabilizing oxygen displacement as predicted in the ZrO<sub>2</sub>–TiO<sub>2</sub> phase diagram.<sup>6</sup> This displacement of oxygen breaks the cubic symmetry and might cause the birefringence as shown in Fig. 3.

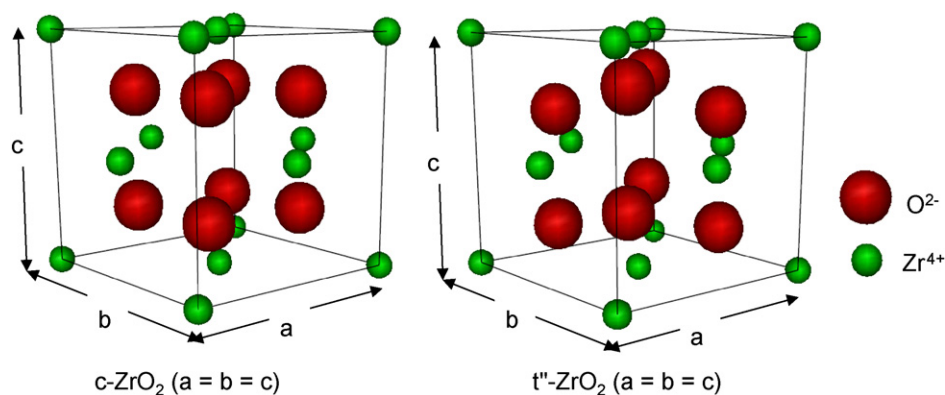
In order to evaluate the influence of yttria content on birefringence of TiO<sub>2</sub>-containing ZrO<sub>2</sub> ceramics, ZrO<sub>2</sub> ceramics with different amount of Y<sub>2</sub>O<sub>3</sub> were prepared.

Raman spectra of the samples with higher Y<sub>2</sub>O<sub>3</sub> content are shown in Fig. 6. The  $470\text{ cm}^{-1}$ , i.e. characteristic for the displacement of oxygen ions, disappeared by additional doping of Y<sub>2</sub>O<sub>3</sub> regardless of the coexistence of TiO<sub>2</sub>.

Probably due to the elimination of oxygen displacement, the birefringence of the TiO<sub>2</sub>-containing ZrO<sub>2</sub> ceramics was drastically reduced as shown in Fig. 7.

The sample with additional 30 wt% Y<sub>2</sub>O<sub>3</sub> (Z10Y–5 wt% TiO<sub>2</sub>–30 wt% Y<sub>2</sub>O<sub>3</sub>, no post-annealing) showed relatively high birefringence ( $\sim 30\text{ nm/cm}$ ) at the rim edge due to the observed residual stress. However, the birefringence of the central region of the sample was 5 nm/cm or below which was comparable with the specification of typical optical glasses.

Fig. 8 shows the in-line and total transmission of the same sample Z10Y–5 wt% TiO<sub>2</sub>–30 wt% Y<sub>2</sub>O<sub>3</sub> shown in Fig. 7. Although slight absorption at 500 to 550 nm probably due to

Fig. 5. Schematic structure of c-ZrO<sub>2</sub> and t''-ZrO<sub>2</sub>.



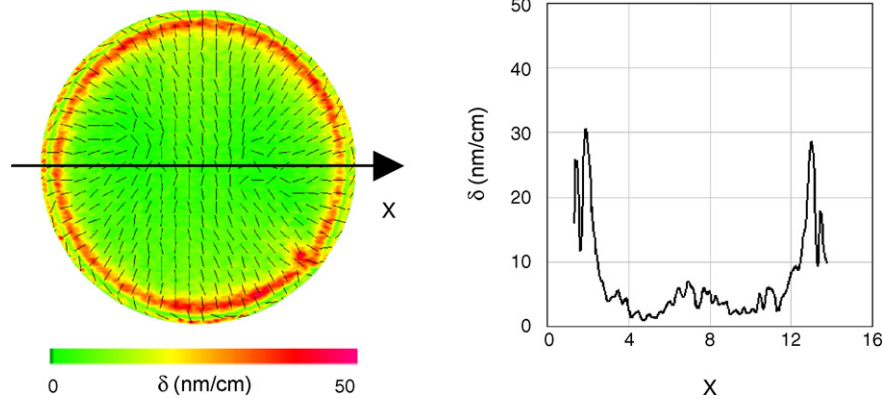


Fig. 7. 2D mapping and 1D profile of the birefringence, cross-Nichols image of Z10Y–5 wt% TiO<sub>2</sub>–30 wt% Y<sub>2</sub>O<sub>3</sub> ceramics.

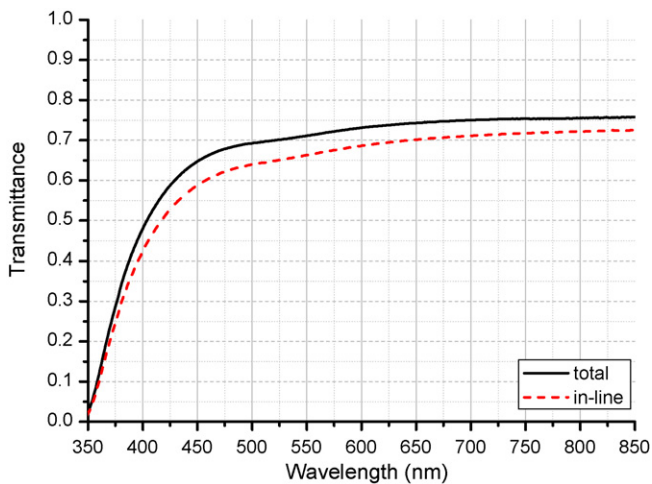


Fig. 8. In-line and total transmission of Z10Y–5 wt% TiO<sub>2</sub>–30 wt% Y<sub>2</sub>O<sub>3</sub> ceramics. Transmission was measured on a 5.76-mm thick specimen.

impurity from the Y<sub>2</sub>O<sub>3</sub> raw powder material, the in-line transmission was improved from ~60% at 600 nm to ~69% at a sample thickness of 5.8 mm by elimination of birefringence and optical scattering through an increased amount of Y<sub>2</sub>O<sub>3</sub> inside the ZrO<sub>2</sub> ceramic.

In Fig. 9 a photograph of Z10Y–5 wt% TiO<sub>2</sub>–30 wt% Y<sub>2</sub>O<sub>3</sub> is presented. The sample shows slight yellowish discoloration



Fig. 9. Picture of Z10Y–5 wt% TiO<sub>2</sub>–30 wt% Y<sub>2</sub>O<sub>3</sub> ceramics (the sample is ~1 cm spaced from the background).

caused by the TiO<sub>2</sub> addition. Considering the requirements for optical materials for lenses these discoloration needs to be removed, consequently, it is preferable to avoid addition of TiO<sub>2</sub> inside ZrO<sub>2</sub> optoceramics.

In Fig. 10 the scattering coefficient calculated from  $k_{\text{in-line}} - k_{\text{total}}$  of the prepared samples is given. Keeping the amount of Y<sub>2</sub>O<sub>3</sub> constant a decrease in scattering is observed

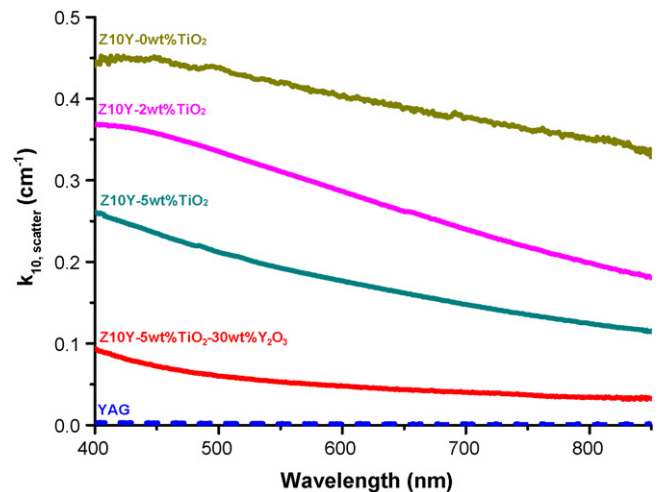


Fig. 10. Scattering coefficient calculated from  $k_{\text{in-line}} - k_{\text{total}}$  of the prepared samples.

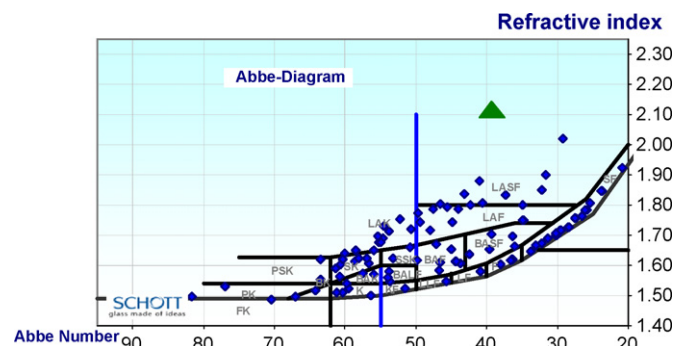


Fig. 11. Position of sample Z10Y–5 wt% TiO<sub>2</sub>–30 wt% Y<sub>2</sub>O<sub>3</sub> in Abbe diagram (triangle).

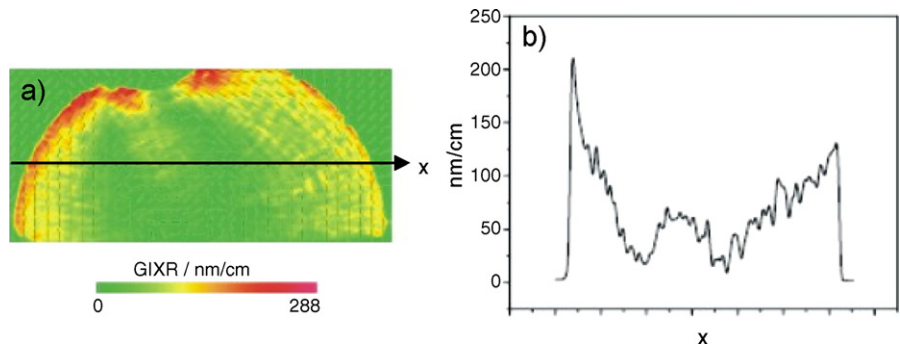


Fig. 12. 2D mapping of birefringence (a) and profile of birefringence along x-axis (b) of Z78.

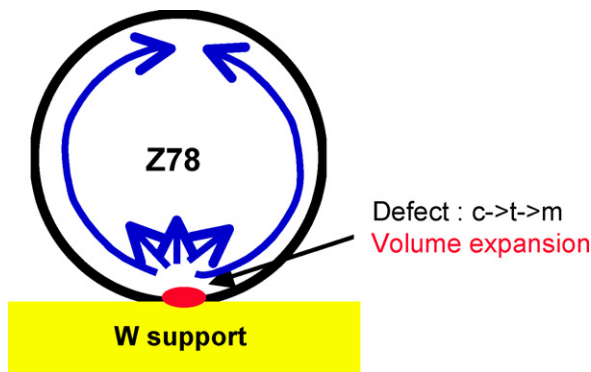


Fig. 13. Possible-induced compression stress by volume expansion at a defect.

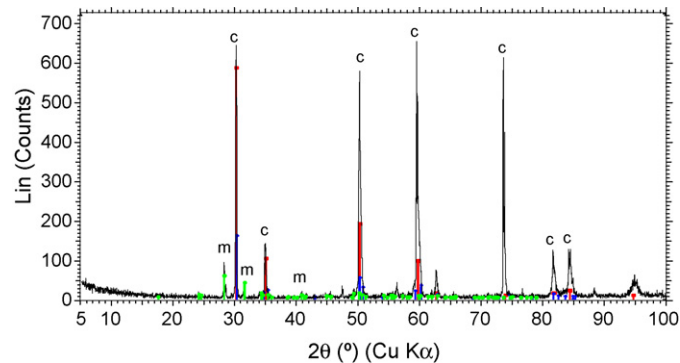


Fig. 14. XRD pattern from the defect on the round surface of Z10Y–5 wt% TiO<sub>2</sub> ceramics which was formed by a at the contact with W support during vacuum sintering. m-ZrO<sub>2</sub> (indicated by m) was detected as well as c-ZrO<sub>2</sub> (marked by c). (For interpretation of the references to color in citation of this figure, the reader is referred to the web version of the article.)

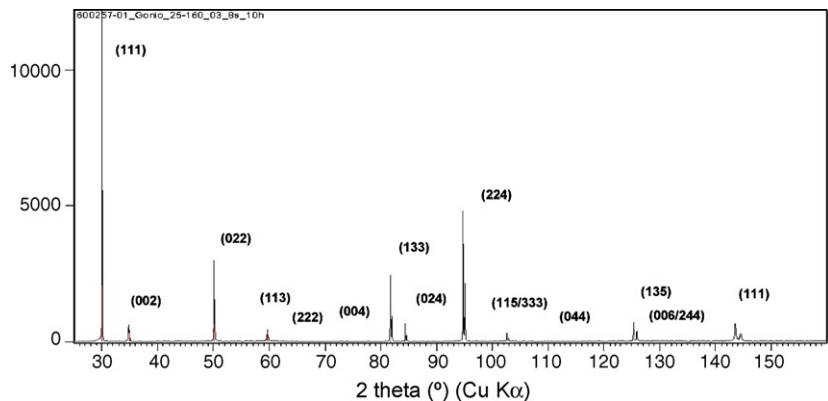


Fig. 15. XRD pattern of Z10Y–5 wt% TiO<sub>2</sub> ceramics (face not in contact with support).

Table 1  
Mol fraction, refractive index at 633 nm, scattering as compared to Konoshima YAG and birefringence of prepared ZrO<sub>2</sub> optoceramics refractive indices have been measured with an accuracy of  $\pm 0.0001$  ( $n_d = (n_{588\text{ nm}} - 1)/(n_{486\text{ nm}} - n_{656\text{ nm}})$ )

Sample	Mol fraction (mol%)			$n$ at 633 nm	$n_d$ at 588 nm	$n$ at 780 nm	Dispersion ( $v_d$ )	Scatter (times YAG)	Birefringence level in centre (nm/cm)
	ZrO <sub>2</sub>	Y <sub>2</sub> O <sub>3</sub>	TiO <sub>2</sub>						
Z10Y–0 wt% TiO <sub>2</sub>	90.0	10.0	0.0	2.161	N.A.	N.A.	N.A.	~260×	5–10
Z10Y–2 wt% TiO <sub>2</sub>	87.0	9.7	3.3	2.177	N.A.	N.A.	N.A.	~185×	10–50
Z10Y–5 wt% TiO <sub>2</sub>	82.7	9.2	8.1	2.196	N.A.	N.A.	N.A.	~115×	50–100
Z10Y–5 wt% TiO <sub>2</sub> –2 wt% Y <sub>2</sub> O <sub>3</sub>	81.6	10.2	8.2	N.A.	N.A.	N.A.	N.A.	N.A.	N.A.
Z10Y–5 wt% TiO <sub>2</sub> –30 wt% Y <sub>2</sub> O <sub>3</sub>	64.2	26.6	9.2	2.1090	2.1176	2.0940	39 ± 1	~ 30×	~5

while incorporating  $\text{TiO}_2$  into the structure. This corresponds to the improvement of microstructure of the samples and confirmed that  $\text{TiO}_2$  is a good sintering aid except for introducing inhomogeneity fluctuations which cause the above discussed birefringence. In the wavelength range between 500 and 800 nm the scatter of the best  $\text{ZrO}_2$  optoceramic (Z10Y–5 wt%  $\text{TiO}_2$ –30 wt%  $\text{Y}_2\text{O}_3$ ) is around  $30\times$  higher than that of ceramic YAG from Konoshima Chemical Co. Ltd. (Japan) or that prepared by Ikesue.<sup>21</sup> The former was qualified for having optical quality. Therefore, a further reduction of scattering by a factor of at least  $10\times$  is needed to be comparable to ceramic YAG (Fig. 10) will be needed to use these optoceramics as lenses and thus needing substantial development efforts in terms of process conditions and additives. Principally, there are still some fine macroscopic “flitters” or patterns observed in all samples by eye that seem to reflect light, i.e. decrease in transmittance and scatter sites.

The refractive index of the prepared  $\text{ZrO}_2$  optoceramics varied between 2.15 and 2.20. By incorporation  $\text{TiO}_2$  into the ceramics, the refractive index increased (Table 1) which is a well known effect in silicate glasses.<sup>22</sup> Increasing the amount of  $\text{Y}_2\text{O}_3$  while keeping the amount of  $\text{TiO}_2$  constant resulted in a decrease in refractive index from 2.20 to 2.11,

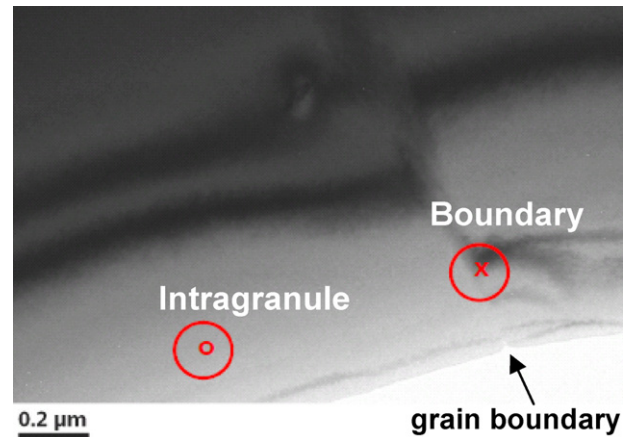


Fig. 16. TEM micrograph of Z10Y–5 wt%  $\text{TiO}_2$  ceramics.

which has also been observed in  $\text{Y}_2\text{O}_3$ -stabilized  $\text{ZrO}_2$  single crystals.<sup>23</sup>

Calculation of reliable dispersion data ( $P_g, F$ ) requires extremely correct refractive index data (5th digit). Nevertheless, a tentative value of  $\sim 39 \pm 1$  for the best  $\text{ZrO}_2$  optoceramic sample (Z10Y–5 wt%  $\text{TiO}_2$ –30 wt%  $\text{Y}_2\text{O}_3$ ) has been calculated

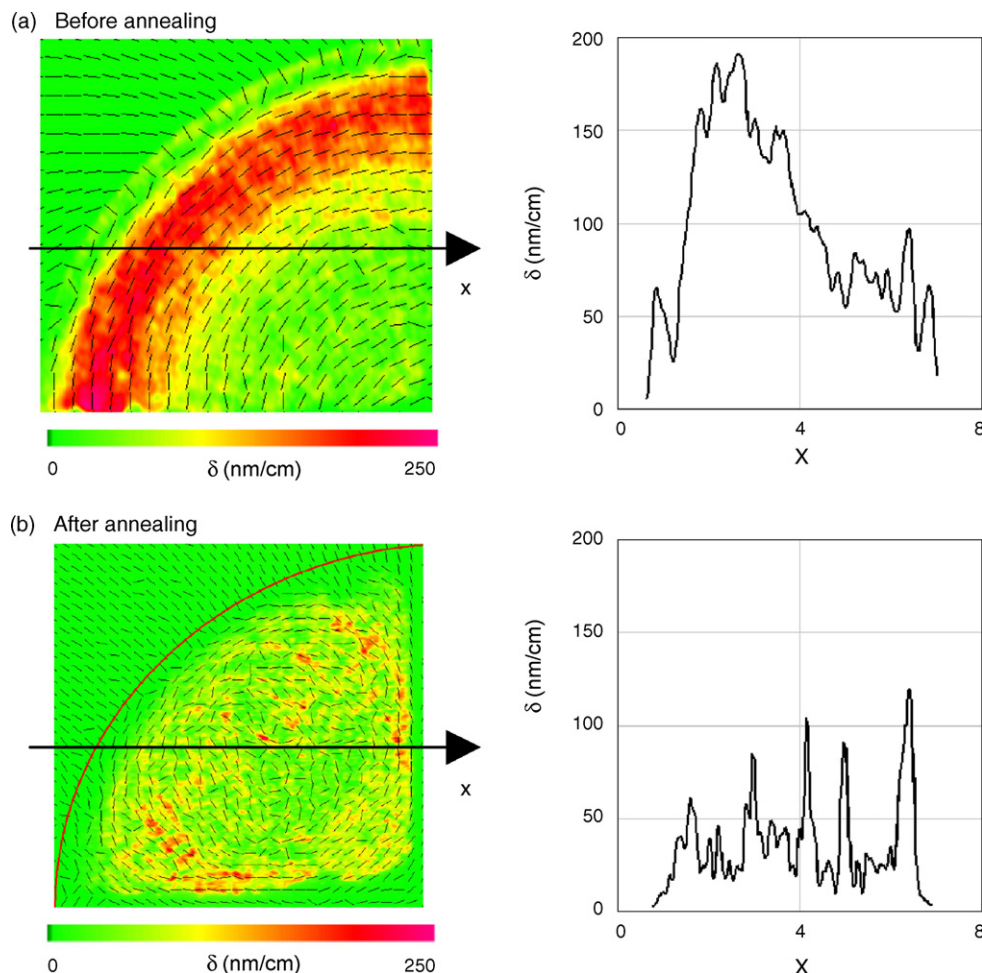


Fig. 17. Birefringence of Z10Y–5 wt%  $\text{TiO}_2$  ceramics before (a) and after (b) post-annealing at 1600 °C for 3 h.

(Fig. 11). Further measurements are currently under way in order to get more accurate refractive index data.

### 3.2. Process related steps influencing transmission and homogeneity

During sintering in the vacuum furnace a whitish ring formed on the outside of the optoceramic samples doped with  $\text{TiO}_2$ . A high intensity of stress birefringence can be observed at the outer rim of the ceramic sample (Fig. 12).

This inhomogeneous distribution of the birefringence starts from a defect at the outer RIM where monoclinic  $\text{ZrO}_2$  (m- $\text{ZrO}_2$ ) could be detected. Thus,  $\text{Y}_2\text{O}_3$  was extracted from c- $\text{ZrO}_2$  by reaction with the W-containing support plate during sintering and during cooling transformation to tetragonal  $\text{ZrO}_2$  (t- $\text{ZrO}_2$ ) and then to m- $\text{ZrO}_2$  occurred.

Volume expansion coming along these phase transformations (c- > t: 2.4 vol%, t- > m: 7.4 vol%) will induce compression stress around the defect and the outer region of the Z10Y–5 wt%  $\text{TiO}_2$  ceramic as shown in Fig. 13. In Fig. 14 the XRD pattern from the defect at the outer rim surface of Z10Y–5 wt%  $\text{TiO}_2$  which is formed by reaction with the W support during vacuum sintering is shown. Monoclinic  $\text{ZrO}_2$  (indicated by green marker) was detected together with c- $\text{ZrO}_2$  (marked by red).

XRD analysis revealed further that only the cubic  $\text{ZrO}_2$  phase developed inside the sample after sintering of the Y-stabilized c- $\text{ZrO}_2$ -containing 5 wt%  $\text{TiO}_2$  (Z10Y–5 wt%  $\text{TiO}_2$ , Fig. 15). Microscopic fluctuation of  $\text{Y}_2\text{O}_3$  and/or  $\text{TiO}_2$  within the ceramic was also checked by energy dispersive X-ray spectrometer equipped on a TEM (Fig. 16). Although slight accumulation of  $\text{TiO}_2$  at grain boundaries by around 1 mol% was detected, no significant deviation of composition generating tetragonal and/or monoclinic  $\text{ZrO}_2$  and/or other  $\text{TiO}_2$  and/or  $\text{Y}_2\text{O}_3$  related compounds, which might cause birefringence, was detected. Nevertheless, besides the structural change, this local concentration of  $\text{TiO}_2$  at grain boundaries could cause strong local fluctuation of refractive index and/or local strains enough to generate the observed scatter.

In conclusion, the actual observed birefringence in the c- $\text{ZrO}_2$  ceramics-containing  $\text{TiO}_2$  is a superimposition of birefringence come from t'- $\text{ZrO}_2$  and also from mechanical/residual stress as described above.

In order to release the residual strain, post-annealing was performed at 1600 °C for 3 h in air using low heating and cooling rates. After post-annealing the high intensity of birefringence at the outer rim of the samples has been drastically reduced. It was confirmed that the birefringence due to residual stress, which was typically appearing at the rim edge of the specimen and whose intensity was higher than 150 nm/cm in the most cases, was clearly eliminated by the annealing as shown in 2D and 1D mappings of Fig. 17. The birefringence in the sample centre is still remaining. So the displacement of oxygen has not been reduced by the post-annealing. Unfortunately, the transmission was degraded by the post-annealing which could be due to bubbles, i.e. evaporation of Ar dissolved in the crystal lattice during HIPing.

## 4. Conclusions

Remarkable progress has been made in the field of transparent ceramics in the past years towards real optical quality. YAG ceramics are already available in qualities close to that of optical glass enabling application as laser host. Nevertheless, sophisticated optical imaging in the UV–vis requires even better “glass like” quality in terms of scattering and optical homogeneity. High refracting tunable materials with  $n_d > 2.0$  (zirconia, perovskites) are interesting for consumer optics. However, the successful and sustainable introduction of a new optical material into the optical industry requires identification and assessment of other/additional uniqueness of optoceramics in terms of their optical properties.

Transparent ceramics have been obtained in the  $\text{ZrO}_2$ – $\text{Y}_2\text{O}_3$ -system using  $\text{TiO}_2$  as sintering agent. Optical properties have been evaluated and a variation of refractive index between 2.10 and 2.20 has been observed, depending upon addition of  $\text{TiO}_2$  as sintering aid.

It has been noted that the addition of  $\text{TiO}_2$  results in the appearance of a yellowish discoloration and of birefringence in the optoceramic samples. However, a decreased  $\text{TiO}_2$  content gives negative impact on the transmission of the sintered body.

Oxygen displacement in c- $\text{ZrO}_2$  crystal structure induced by addition of  $\text{TiO}_2$  and residual stress induced during sintering and post-oxidation process was suggested as the origins of the birefringence. Post-annealing was effective to relax the residual stress at the outer rim edge of the samples and thus reduced the birefringence induced by this stress. But through this process no reduction of birefringence in the sample centres could be obtained. This centre birefringence has been determined to be caused by oxygen displacement in c- $\text{ZrO}_2$  lattice. Nevertheless, a post-annealing treatment is not a practical measure to remove the birefringence, because at the same time transmission is degraded.

Increasing the amount of  $\text{Y}_2\text{O}_3$  without changing the  $\text{TiO}_2$  contents resulted in a decrease of birefringence in the sample centre, thus eliminating the oxygen displacement in the  $\text{ZrO}_2$  ceramics-containing  $\text{TiO}_2$ .

In order to improve the optical quality of the  $\text{ZrO}_2$  transparent ceramics needs substantial development efforts in terms of (a) avoidance of contamination of the sample through the support material of the sample in vacuum sintering furnace, i.e. change the support from W to  $\text{ZrO}_2$  and thus avoiding possible chemical reaction of W with sample; (b) change heating elements in HIP (avoid effect of pollution effects); (c) improvement of the sintering, and post-sintering heat treatment processes which are related to the induction of residual stresses in the ceramic and use of different; (d) usage of different additives instead of  $\text{TiO}_2$ .

## References

1. Yoshida, K., Yabe, T., Uchida, S., Ikesue, A. and Kamimura, T., New trends on solid-state lasers. *AIP Conf. Proc.*, 2006, **830**, 14–20.
2. Kvatchadze, V., Kalabegishvili, T., Vylet, V., Abramishvili, M., Akhvlediani, Z., Galustashvili, M., Garibashvili, K. and Sobolevskaya, S., Ceramic  $\text{MgO}:\text{LiF}$ : promising material for selective detector. *Radiat. Eff. Defects*, 2006, **161**(5), 305–311.



3. Greskovich, C. and Wood, K. N., Fabrication of transparent  $\text{ThO}_2$ -doped  $\text{Y}_2\text{O}_3$  ceramics. *Am. Ceram. Soc. Bull.*, 1973, **52**(5), 473–478.
4. Coble, R. L., Sintering crystalline solids. Part I. Intermediate and final state diffusion models. *J. Am. Ceram. Soc.*, 1961, **32**, 787–792.
5. Ikesue, A. and Furusato, I., Fabrication of polycrystalline, transparent YAG ceramics by a solid-state reaction method. *J. Am. Ceram. Soc.*, 1995, **78**(1), 225–228.
6. Ikesue, A. and Kamata, K., Microstructure and optical properties of hot isostatically pressed Nd:YAG ceramics. *J. Am. Ceram. Soc.*, 1996, **79**, 1927–1933.
7. Sube, M., Masayoshi, Yukio, K. H., Mitsuru, S., Katsube, M., Higuchi, Y. and N. Tanaka, Transparent ceramic and method for production thereof, and optical element, JP3882504B2, 2000.
8. Tsukuma, K., Kubota, Y. and Tsukidate, T., Transparent  $\text{ZrO}_2$ – $\text{Y}_2\text{O}_3$ – $\text{TiO}_2$  ceramics. *Advances in Ceramics, Science and Technology of Zirconia*, vol. 24., 1988, p. 287.
9. Tsukuma, K., Transparent titania–yttria–zirconia ceramics. *J. Mater. Sci. Lett.*, 1986, **5**, 1143–1144.
10. Radford, K. C. and Bratton, R. J., Zirconia electrolyte cells. Part I. Sintering studies. *J. Mater. Sci.*, 1979, **14**, 59–65.
11. Matsui, K., Ohmichi, N., Ohgai, M., Yoshida, H. and Ikuhara, Y., Grain boundary segregation induced phase transformation in yttria stabilized tetragonal zirconia polycrystal. *J. Ceram. Soc. Jpn.*, 2006, **114**(1327), 230–237.
12. Braun, A., Clasen, R., Oetzel, C. and Wolff, M., In *Hochleistungskeramik aus Nanopulvermischungen für optische und dentale Anwendungen*, Vol. 20, ed. A. Roosen, Fortschrittsberichte der Deutschen Keramischen Gesellschaft, Band, Heft 1, 2006, pp. 131–136, ISSN: 0173-9913.
13. Wolff, M., Clasen, R. et al., Investigation on the transparent polycrystalline zirconia, cfi/Ber. DKG, 2005, **82**(13), 166–169.
14. Klimke, J. and Krell, A., *Polycrystalline  $\text{ZrO}_2$ —Transparent Ceramics with High Refractive Index*, Fraunhofer IKTS, Annual Report, Department: Materials, 2005, p. 23.
15. Apetz, R. and van Bruggen, M. P. B., Transparent alumina: a light scattering model. *J. Am. Ceram. Soc.*, 2003, **86**(3), 480–486.
16. Lee, H. J., Henry, C. H., Orlowsky, K. J., Kazarinov, R. F. and Kometani, T. Y., Refractive index dispersion of phosphosilicate glass, thermal oxide, and silicon nitride films on silicon. *Appl. Opt.*, 1988, **27**, 4104.
17. *Schott Technical Information*, TIE-29: Refractive Index and Dispersion, 2007.
18. Dericiogluet, A. F., Boccaccini, A. R., Dlouhy, I. and Kagawa, Y., Effect of chemical composition on the optical properties and fracture toughness of transparent magnesium aluminate spinel ceramics. *Mater. Trans.*, 2005, **46**(5), 996–1003.
19. Yashima, M., Ishizawa, N. and Yoshimura, M., High-temperature X-ray study of the cubic-tetragonal diffusionless phase transition in the  $\text{ZrO}_2\text{ErO}_{1.5}$  system. Part I. Phase change between two forms of a tetragonal phase,  $t'$ - $\text{ZrO}_2$  and  $t''$ - $\text{ZrO}_2$ , in the compositionally homogeneous 14 mol%  $\text{ErO}_{1.5}$ - $\text{ZrO}_2$ . *J. Am. Ceram. Soc.*, 1993, **76**, 641–648.
20. Zhou, Y., Lei, T.-C. and Sakuma, T., Diffusionless cubic-to-tetragonal phase transition and microstructural evolution in sintered zirconia–yttria ceramics. *J. Am. Ceram. Soc.*, 1991, **74**(3), 633–640.
21. Ikesue, A., personal communication.
22. Suzuki, H., Taira, M., Wakasa, K. and Yamaki, M., Refractive-index-adjustable fillers for visible-light-cured dental resin composites. *J. Dental Res.*, 1991, **70**, 883–888.
23. Wood, D. L., Nassau, K. and Kometani, T. Y., Refractive index of  $\text{Y}_2\text{O}_3$  stabilised cubic zirconia: variation with composition and wavelength. *Appl. Opt.*, 1990, **29**(16), 2485–2487.